Astron. Astrophys. 340, L19–L22 (1998)

ASTRONOMY AND ASTROPHYSICS

LETTER

Letter to the Editor

The extraordinary X-ray spectrum of XTE J0421+560

A. Orr[1], A.N. Parmar[1], M. Orlandini[2], F. Frontera[2,3], D. Dal Fiume[2], A. Segreto[4], A. Santangelo[4], and M. Tavani[5,6]

[1] Astrophysics Division, Space Science Department of ESA, ESTEC, 2200 AG Noordwijk, The Netherlands
[2] Istituto Tecnologie e Studio Radiazioni Extraterrestri, CNR, Via Gobetti 101, I-40129 Bologna, Italy
[3] Dipartimento di Fisica, Università di Ferrara, Via Paradiso 11, I-44100 Ferrara, Italy
[4] Istituto di Fisica Cosmica ed Applicazioni all'Informatica, CNR, Via U. La Malfa 153, I-90146 Palermo, Italy
[5] Columbia Astrophysics Laboratory, Columbia University, 538 West 120th Street, New York, NY 10027, USA
[6] Istituto di Fisica Cosmica e Tecnologie Relative, CNR, Via Bassini 15, I-20133 Milano, Italy

Received 2 September 1998 / Accepted 18 October 1999

Abstract. We report results of two BeppoSAX observations of the transient X-ray source XTE J0421+560 during the outburst that started in March 1998. The source exhibits radio jets and coincides with the binary system CI Cam. The 0.1–50 keV spectrum is unlike those of other X-ray transients, and cannot be fit with any simple model. The spectra can be represented by an absorbed two component bremsstrahlung model with narrow Gaussian emission features identified with O, Ne/Fe-L, Si, S, Ca and Fe-K. During the second observation (TOO2) the energies of the O and the Ne/Fe-L features decreased smoothly by $\sim$9% over an interval of 30 hrs. No significant energy shift of the other lines is detected with e.g, a 90% confidence upper limit to any Fe-K line shift of 3.5%. No moving lines were detected during the first observation (TOO1) with e.g., an upper limit of $<$1.4% to any shift of the Fe-K line. The low-energy absorption decreased by a factor $\geq$1.8 from $\sim 6 \times 10^{21}$ atom cm^{-2} between TOO1 and TOO2. We propose that the time variable emission lines arise in precessing relativistic jets, while the stationary lines originate in circumstellar material.

Key words: stars: binaries — stars: emission-line, Be – stars: individual (XTE J0421+560) – stars: novae – X-rays: stars

1. Introduction

Relativistic galactic jet sources are usually seen in X-ray binaries, where a black hole or neutron star is accreting from a "normal" star. Recently a new galactic jet source, XTE J0421+560, was discovered by the Rossi-XTE satellite as a bright and rapidly rising X-ray transient on 1998 March 31 (Smith et al. 1998). The source reached a peak intensity of $\sim$2 Crabs on April 1, before rapidly decaying. Radio observations quickly allowed the identification of the optical counterpart with the binary system CI Cam (= MWC 84). Miroshnichenko (1995) and Bergner et al. (1995) model CI Cam as a K0 II–B0 V system embedded in a hot circumstellar dust shell. Chkhikvadze (1970) estimates the interstellar extinction (1.5 mag.) and the distance (1 kpc) of CI Cam. Optical spectra before and after the outburst exhibit strong Balmer and He I emission lines (Merrill 1933). He II lines appeared after the outburst (Wagner & Starrfield 1998). Within a week of the X-ray outburst, extended radio emission appeared in the form of an S-shaped jet. If the X-ray and radio outbursts are assumed contemporaneous, for a distance of 1 kpc, the rate of expansion of the radio emission implies a tangential velocity of 0.15 c (Hjellming & Mioduszewski 1998).

In this *Letter* we describe the BeppoSAX spectra of XTE J0421+560 in the days following the 1998 March 31 outburst. X-ray and optical timing analysis and light curves are presented in Frontera et al. (1998).

2. Observations and data reduction

Data from the Low-Energy Concentrator Spectrometer (LECS; 0.1–10 keV), Medium-Energy Concentrator Spectrometer (MECS; 1.3–10 keV) High Pressure Gas Scintillation Proportional Counter (HPGSPC; 5–120 keV) and the Phoswich Detection System (PDS; 15–300 keV) on-board BeppoSAX (Boella et al. 1997) are presented. All these instruments are co-aligned and collectively referred to as the Narrow Field Instruments, or NFI.

XTE J0421+560 was observed twice by BeppoSAX as a target of opportunity (TOO). TOO1 took place between 1998 April 3 05:03 and 17:44 and TOO2 between 1998 April 9 00:48 and April 10 06:49 UTC. The data were processed using the SAXDAS 1.3.0 package. The TOO1 exposures are 6.8, 21.5, 9.8, and 9.3 ks in the LECS, MECS, HPGSPC, and PDS, respectively. The corresponding count rates are 6.8, 12.7, 9.5, and 2.2 s^{-1}. The TOO2 exposures are 10.7, 47.0, and 17.8 ks in the LECS, MECS, and HPGSPC. The corresponding count rates are 16.5, 0.8, and 0.2 s^{-1}. LECS and MECS data were extracted centered on the position of XTE J0421+560 using radii of 8′ and 4′, respectively. Background subtraction in the imaging instruments

Send offprint requests to: aparmar@astro.estec.esa.nl

Table 1. Results of fits to the BeppoSAX NFI spectra. Model code: PL = power-law; CO PL = cut-off power-law; BKNPL = broken power-law; DBBPL = disk blackbody + power-law; 2BRMS = double bremsstrahlung; 2MEKAL = double MEKAL. Except for the 2MEKAL model, emission lines fixed at the energies given in Table 2 are included. The cut-off and break energies are listed for the CO PL and BKNPL models, respectively. The metal abundance "Fe/He" with respect to solar is given for the 2MEKAL model. N_H is in units of 10^{21} atom cm^{-2}, kT and E are in keV

	TOO1				TOO2			
Model	N_H	kT, $E_{co,br}$	Γ, Fe/He	χ^2_ν/dof	N_H	kT, $E_{co,br}$	Γ, Fe/He	χ^2_ν/dof
PL	16.3 ± 0.4	...	2.58 ± 0.01	5.3/719	2.0 ± 0.1	...	3.08 ± 0.02	5.19/495
CO PL	6.0 ± 0.2	7.6 ± 0.3	1.53 ± 0.03	1.23/718	2.0 ± 0.1	>135	3.07 ± 0.02	5.21/493
BKNPL	16.5 ± 0.4	1.00 ± 0.03	$11.3 \pm {}^{1.5}_{1.2}$	5.2/717	3.2 ± 0.1	1.84 ± 0.04	5.54 ± 0.09	1.64/492
	...	...	2.58 ± 0.01		...	...	2.94 ± 0.03	
DBBPL	10.2 ± 0.6	2.59 ± 0.07	2.72 ± 0.04	1.28/717	3.3 ± 0.1	1.42 ± 0.03	5.8 ± 0.1	1.55/492
2BRMS	$6.0 \pm {}^{0.6}_{0.4}$	$1.27 \pm {}^{0.41}_{0.28}$	...	1.24/717	3.0 ± 0.1	0.20 ± 0.01	...	1.51/492
	...	$6.81 \pm {}^{0.21}_{0.17}$	...		...	$2.78 \pm {}^{0.07}_{0.09}$		
2MEKAL	10.8 ± 0.4	0.81 ± 0.05	0.45 ± 0.02	1.44/721	$0.94 \pm {}^{0.04}_{0.06}$	0.319 ± 0.004	0.64 ± 0.04	16.7/496
	...	6.18 ± 0.09	...		...	$3.85 \pm {}^{0.10}_{0.12}$	...	

was performed using standard files, but is not critical for such a bright source. Background subtraction in the non-imaging instruments was carried out using data from offset intervals.

3. The average X-ray spectra

Spectral analysis was performed separately on the average TOO1 and TOO2 NFI spectra. Spectra were selected in the energy ranges 0.3–10 keV, 1.8–10 keV, 5–20 keV and 15–50 keV for the LECS, MECS, HPGSPC and PDS, respectively. For TOO2 only an upper limit from the PDS in the 15–50 keV energy range was obtained, since the source was much fainter $\gtrsim$10 keV than in TOO1. Factors were included in the spectral fitting to allow for known normalization differences between the instruments. Uncertainties and upper limits are quoted at 90% confidence throughout. Fit results are listed in Tables 1 and 2. No simple model, e.g. absorbed power-law, broken or exponentially cut-off power-law, thermal bremsstrahlung, or multi-temperature disk blackbody (Mitsuda et al. 1984) plus power-law, gives a satisfactory fit to either observation. This last model has been successfully fit to the spectra of many soft X-ray transients (e.g., Tanaka & Lewin 1995). Inspection of the residuals reveals the presence of strong emission lines in the spectra. Including such features in the models brings a significant, albeit insufficient, improvement in fit quality. The description of the lines is given in Table 2. All fitted lines are narrow and unresolved by the LECS and MECS. However a blend of narrow lines cannot be excluded. If allowed to vary, the Gaussian widths, σ, remain small compared to the instrument resolution and the fit statistics do not change significantly. Therefore σ was fixed at 0.1 keV.

The best fit for TOO1 is obtained using a cut-off power-law with narrow Gaussian emission features. The fit is formally unacceptable with a χ^2 of 1.23, for 718 degrees of freedom (dof), but models the overall shape of the 1–20 keV spectrum reasonably well. Next best is a model consisting of two thermal bremsstrahlung components plus emission lines. The observed TOO1 fluxes $F_{0.5-2}$ and F_{2-10} are 0.3 and 1.0×10^{-9} ergs cm^{-2} s^{-1}. At a distance of 1 kpc these correspond to luminosities of 3.4×10^{34} and 1.2×10^{35} erg s^{-1}.

Table 2. Two bremsstrahlung and narrow Gaussian emission lines model fits to XTE J0421+560. The O VIII and Ne X features in TOO2 are assumed to be blue-shifted from their rest energies of 0.65 and 1.02 keV (see text)

Parameter	TOO1	TOO2	Ident.
N_H (10^{21} cm^{-2})	$6.0 \pm {}^{0.6}_{0.5}$	$3.0 \pm {}^{0.7}_{0.4}$	
kT_1 (keV)	$1.30 \pm {}^{0.60}_{0.30}$	$0.20 \pm {}^{0.01}_{0.02}$	
kT_2 (keV)	$6.82 \pm {}^{0.26}_{0.19}$	$2.78 \pm {}^{0.07}_{0.04}$	
E_{line} (keV)	0.74	$0.740 \pm {}^{0.005}_{0.008}$	O VIII Kα
EW (eV)	<45	$1420 \pm {}^{525}_{240}$	
E_{line} (keV)	0.99 ± 0.02	$1.155 \pm {}^{0.004}_{0.003}$	Ne X Kα
EW (eV)	$163 \pm {}^{55}_{36}$	$635 \pm {}^{37}_{27}$	Fe-L
E_{line} (keV)	1.91 ± 0.02	1.86 ± 0.03	Si XIII Kα
EW (eV)	65 ± 8	105 ± 21	
E_{line} (keV)	2.50 ± 0.03	2.47 ± 0.03	S XV Kα
EW (eV)	38 ± 7	$89 \pm {}^{25}_{17}$	
E_{line} (keV)	6.73 ± 0.01	6.75 ± 0.03	Fe XXV Kα
EW (eV)	597 ± 18	731 ± 72	
χ^2_ν (dof)	1.24 (714)	1.53 (487)	

The X-ray spectrum of XTE J0421+560 changed dramatically between TOO1 and TOO2 (see Fig. 1) with the appearance of strong soft emission at $\lesssim$1 keV. All the models listed in Table 1 show a reduction in N_H of at least a factor $\geq$1.8 between TOO1 and TOO2. Such a change may result from obscuration by material in an expanding shell. The best description of the TOO2 data is achieved with a double bremsstrahlung model including narrow Gaussian emission lines. The observed TOO2 fluxes $F_{0.5-2}$ and F_{2-10} are 1.7 and 0.05 $\times 10^{-9}$ ergs cm^{-2} s^{-1}.

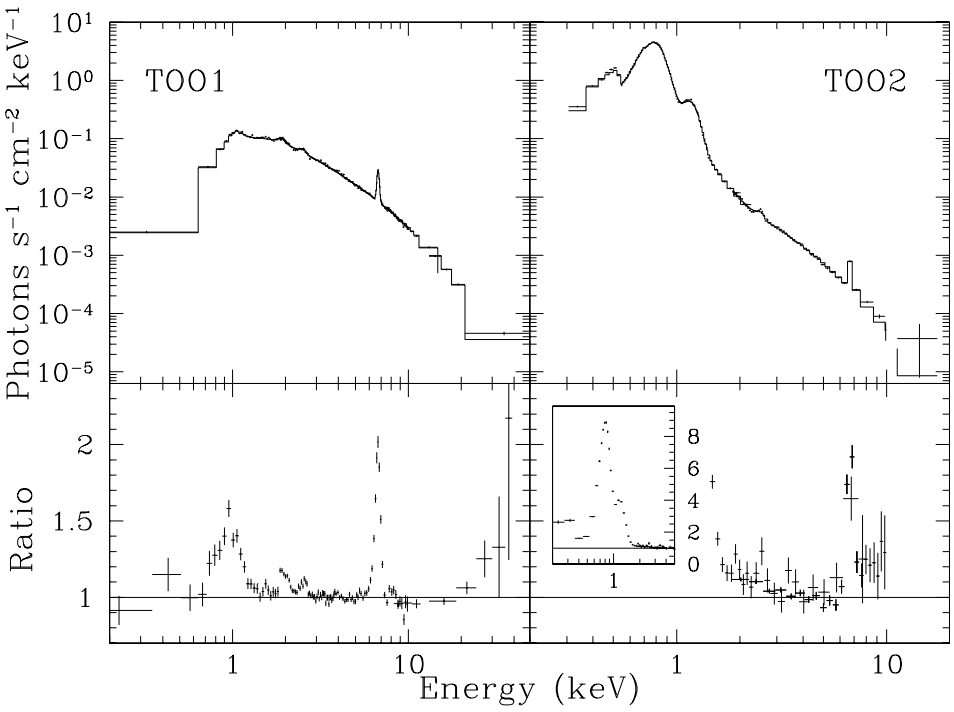

Fig. 1. *Top*: Deconvolved photon spectra of XTE J0421+560 during TOO1 and TOO2 using two bremsstrahlung components plus emission lines (see Table 2). *Bottom*: data to model ratios, where the line normalizations are set equal to zero in the models. The inset shows the TOO2 model ratio near 1 keV where there is strong soft emission

The double MEKAL model, which fits the TOO1 spectrum reasonably well, provides a very poor fit to TOO2.

The double bremsstrahlung plus narrow emission lines model gives a reasonable and "simple" parameterization of both spectra and was therefore chosen to compare TOO1 and TOO2. Table 2 shows that the continuum temperatures decreased significantly between TOO1 and TOO2. Features at 1.9, 2.5 and 6.7 keV, identified with He-like Kα emission from Si, S, and Fe, are observed in both spectra. There are no large changes in their equivalent widths, EW, or mean energies between the observations. In TOO1 a feature is present at 0.99 keV with an EW of 163 eV. This may be identified with Kα emission from Ne X and/or a number of Fe-L transitions. In TOO2 intense features are present at 0.74 and 1.15 keV with EWs of 1420 and 635 eV, respectively. There are no prominent emission lines with energies close to 0.74 keV. However, if the 1.15 keV feature is interpreted as the Doppler shifted Ne X/Fe-L complex (observed at 0.99 keV in TOO1), and if the 0.74 keV feature is also Doppler shifted by the same amount, its rest energy is 0.63 keV – close to the energy of the prominent O VIII line at 0.65 keV. We therefore tentatively identify the TOO2 0.74 keV feature with blue-shifted O VIII emission. The upper limit to a Gaussian emission feature at 0.65 keV during TOO1 is 36 eV. Finally, the TOO1 fits improve significantly (at 99% confidence using the F-statistic) when a Ca XIX line is included at 3.9 keV. However, the EW is small (16 ± 7 eV) and this line is not required in TOO2.

4. Time resolved spectral analysis

The data from TOO1 and TOO2 were divided into 8 and 5 time intervals, respectively, and fitted with the double bremsstrahlung and narrow emission line model (see Table 2). During TOO1 the line parameters (EW and energy, if left free) do not vary significantly between the intervals. The upper limit to any 6.7 keV line shift is 1.4%. The column density, N_H, remains approximately constant. The fluxes of the different model components were calculated for each interval. No significant variation of the fluxes is measured, except that of the hard bremsstrahlung component and the 6.7 keV line, which both decrease smoothly by a factor $\sim$1.8.

During the 30 hr observation of TOO2 the energies of the 0.74 and 1.15 keV lines, tentatively identified as blue-shifted O VIII and Ne X/Fe L emission, respectively, both display a regular and significant decrease by $7.7\pm^{1.1}_{2.1}$% and $9.6\pm^{1.3}_{2.4}$%. Changes in the underlying continuum are unlikely to be responsible for these shifts but cannot be excluded. There is no significant change in N_H, or the energies, fluxes, and EWs of the 1.9, 2.5 and 6.75 keV lines. The upper limit to any shift in the 6.75 keV line is 3.5%. The fluxes in the soft and hard bremsstrahlung components decrease by factors 1.3 and 3, and the fluxes in the two soft lines decrease by a factor 1.8. The EWs of the two soft lines increase then decrease (see Fig. 2). Fig. 3 shows the change in energy of the 0.74 keV line during TOO2.

5. Discussion

The X-ray spectra of XTE J0421+560 presented here are unlike those of any other X-ray transient. Certain properties are reminiscent of the galactic radio jet source SS 433 (e.g. the appearance of a twisted radio-jet after the outburst, the presence of shifting emission lines and the X-ray luminosities; see also Frontera et al. (1998)). The X-ray spectrum of SS 443 displays a pattern of red- and blue-shifted He- and H-like emission

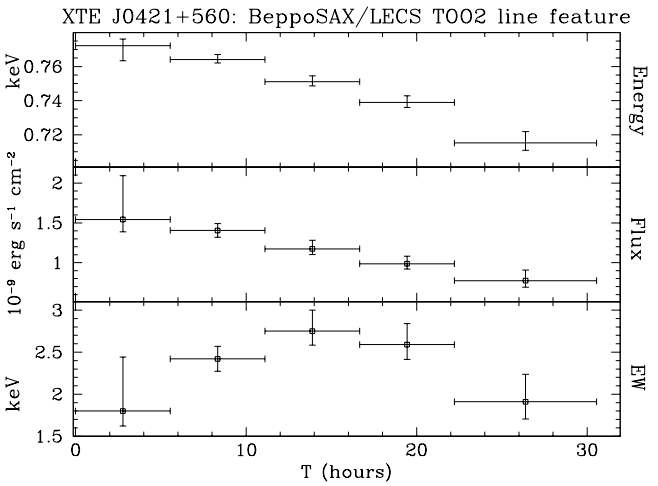

Fig. 2. The variation in energy, flux and EW of the 0.74 keV feature during TOO2. The variations in these parameters for the 1.15 keV feature are almost identical

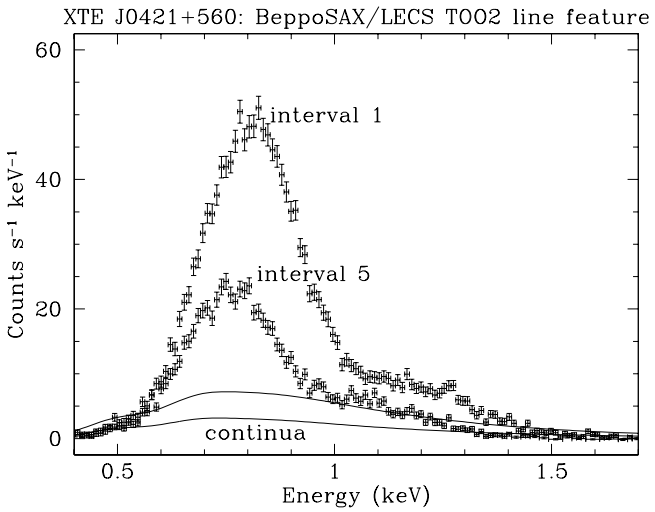

Fig. 3. The change in the 0.74 keV feature between TOO2 intervals 1 and 5. The two solid lines show the subtracted continua, changes in which cannot account for the observed shift

lines superposed on a two temperature bremsstrahlung continuum (Kotani et al. 1994). The lines most probably originate in two collimated precessing (with a period of 163 d) relativistic ($0.26\,c$) jets which result from super-Eddington accretion onto a black hole (e.g., Rose 1995). We propose that the time variable features in XTE J0421+560 also originate in jets and that the variation in energy of these features is due to precession. Fitting a sinusoid to the variation in energy of the 0.74 keV feature during TOO2 and assuming a rest energy of 0.65 keV (ie. that the line is O VIII Kα) implies a precessional period of $\geq$6 days and a velocity of $0.20 \pm {}^{0.08}_{0.01}\ c$ (1σ uncertainty).

ASCA observations of some high mass X-ray binary pulsars such as Vela X-1 (Nagase et al. 1994) reveal spectra rich in He-like emission lines, almost certainly due to reprocessing in circumstellar material. The stationary lines (Si XIII, S XV, Fe XXV, and possibly Ca XIX) most probably originate in circumstellar matter. The identification of the moving features with emission from H-like ions (although the rest energies are uncertain), and the stationary ones with He-like ions, is consistent with this interpretation. In the case of SS 443 two sets of moving X-ray lines are seen (Kotani et al. 1994), although earlier studies had revealed only one (e.g, Watson et al. 1986). This was explained by assuming that one beam was occulted by the accretion disk at certain precession phases (Stewart et al. 1987). This may also be the case in XTE J0421+560.

Acknowledgements. AO acknowledges an ESA Fellowship. The BeppoSAX satellite is a joint Italian and Dutch programme.

References

Bergner Y., Miroshnichenko A., Yudin R., et al., 1995, A&AS 112, 221
Boella G., Butler R.C., Perola G.C., et al., 1997, A&AS 122, 299
Chkhikvadze J., 1970, Astrofizika 6, 65
Frontera F., Orlandini M., Amati L., et al., 1998, A&A, this journal
Hjellming R., Mioduszewski A., 1998, IAU Circ. 6872
Kotani T., Kawai N., Aoki T., et al., 1994, PASJ 46, L147
Merrill P., 1933, ApJ 77, 44
Miroshnichenko A., 1995, Astron. and Astrophys. Trans. 6, 251
Mitsuda K., Inoue H., Koyama, K., et al., 1984, PASJ 36, 741
Nagase F., Zylstra G., Sonobe T., et al., 1994, ApJ 436, L1
Rose W.K., 1995, MNRAS 276, 1191
Smith D. Remillard R., Swank J., Takeshima T., Smith E., 1998, IAU Circ. 6855
Stewart G.C., Watson M.G., Matsuoka M., 1987, MNRAS 228, 293
Tanaka K., Lewin W.H.G., 1995, Black-hole binaries. In: Lewin W.H.G., van Paradijs J., van den Heuvel E.P.J. (eds.) X-ray Binaries. Cambridge Univ. Press, Cambridge, p. 121
Wagner R., Starrfield S., 1998, IAU Circ. 6857
Watson M.G., Stewart G.C., Brinkmann A., King A.R., 1986, MNRAS 222, 261